Human Molecular Genetics, 2003, Vol. 12, No. 19 **2519–2532**
DOI: 10.1093/hmg/ddg267

Increased expression of the glial glutamate transporter EAAT2 modulates excitotoxicity and delays the onset but not the outcome of ALS in mice

Hong Guo[1,†], Liching Lai[1,†], Matthew E.R. Butchbach[1,2,†], Michael P. Stockinger[1,†], Xiu Shan[1,3], Georgia A. Bishop[1,3,4] and Chien-liang Glenn Lin[1,2,3,4,*]

[1]Department of Neuroscience, [2]Ohio State Biochemistry Program, [3]Neuroscience Graduate Studies Program and [4]Integrated Biomedical Sciences Graduate Program, The Ohio State University, 4068 Graves Hall, 333 W. 10th Avenue, Columbus, OH 43210, USA

Received May 20, 2003; Revised July 19, 2003; Accepted July 30, 2003

The glial glutamate transporter EAAT2 is primarily responsible for clearance of glutamate from the synaptic cleft and loss of EAAT2 has been previously reported in amyotrophic lateral sclerosis (ALS) and Alzheimer's disease. The loss of functional EAAT2 could lead to the accumulation of extracellular glutamate, resulting in cell death known as excitotoxicity. However, it is still unknown whether it is a primary cause in the cascade leading to neuron degeneration or a secondary event to cell death. The goals of this study were to generate transgenic mice overexpressing EAAT2 and then to cross these mice with the ALS-associated mutant *SOD1(G93A)* mice to investigate whether supplementation of the loss of EAAT2 would delay or rescue the disease progression. We show that the amount of EAAT2 protein and the associated Na^+-dependent glutamate uptake was increased about 2-fold in our *EAAT2* transgenic mice. The transgenic EAAT2 protein was properly localized to the cell surface on the plasma membrane. Increased EAAT2 expression protects neurons from L-glutamate induced cytotoxicity and cell death *in vitro*. Furthermore, our *EAAT2/G93A* double transgenic mice showed a statistically significant (14 days) delay in grip strength decline but not in the onset of paralysis, body weight decline or life span when compared with *G93A* littermates. Moreover, a delay in the loss of motor neurons and their axonal morphologies as well as other events including caspase-3 activation and SOD1 aggregation were also observed. These results suggest that the loss of EAAT2 may contribute to, but does not cause, motor neuron degeneration in ALS.

INTRODUCTION

Excitatory neurotransmission in the mammalian central nervous system (CNS) is mediated in large part by glutamate. Overactivation of glutamatergic neurons can result in a neurodegenerative process known as excitotoxicity (1). Excitotoxic cell death can occur in the immature as well as the mature CNS and shares features with both apoptosis and necrosis (2,3). Excitotoxicity has been implicated as the mechanism of neuronal damage resulting from acute insults such as stroke, epilepsy and trauma as well as during the progression of adult-onset neurodegenerative disorders such as amyotrophic lateral sclerosis (ALS), Alzheimer's disease and Huntington's disease (4).

ALS is a fatal neuromuscular disorder that is characterized by progressive motor dysfunction resulting from selective degeneration of cortical motor neurons and spinal motor neurons. Familial ALS (FALS) accounts for 5–10% of all reported cases of ALS and demonstrates an autosomal dominant pattern of inheritance (5,6). About 25% of the cases of FALS are linked to mutation in gene encoding the antioxidant enzyme Cu^{2+}/Zn^{2+} superoxide dismutase (SOD1). Over 90 distinct familial SOD1 mutations have been found to date (7). Overexpression of some of these ALS-linked mutant SOD1 proteins (i.e. G93A, G37R and G85R) in transgenic mice results in the development of a neurological disorder that resembles ALS (8–10). Several studies have demonstrated that mutant

---

*To whom correspondence should be addressed. Tel: +1 6146885433; Fax: +1 6146888742; Email: lin.492@osu.edu

[†]The authors wish it to be known that, in their opinion, the first four authors should be regarded as joint First Authors.

Human Molecular Genetics, Vol. 12, No. 19 © Oxford University Press 2003; all rights reserved

SOD1 causes motor neuron degeneration by acquiring a toxic gain of function property rather than by the loss of enzymatic activity (9,11,12). The molecular mechanisms underlying mutant SOD1-linked FALS remain unclear.

Glutamate mediated excitotoxicity is postulated to play a major role in motor neuron degeneration (13). Glutamate is normally cleared from the synaptic space by a family of Na^+- and K^+-coupled excitatory amino acid transporters (EAATs) (14). The glial transporter EAAT2 has been shown to be the main mediator of glutamate clearance (15). Early studies showed an increase in the concentration of glutamate in the cerebrospinal fluid of patients with ALS as well as a defect in glutamate transport activity in the motor cortex and spinal cord of ALS patients (16,17). A selective loss of EAAT2 was found in affected regions within the CNS of ALS patients (18). Interestingly, numerous abnormally spliced EAAT2 mRNAs have been identified from the affected areas of ALS patients and the expression of these abnormally spliced RNA species correlated with the loss of EAAT2 protein in ALS (19).

The loss of EAAT2 expression and function is not unique to ALS. Defective glutamate transport and loss of EAAT2 protein have also been observed in affected brain regions of Alzheimer's disease patients (20,21). The expression of EAAT2 was reduced in an age-dependent manner in a mouse model for Huntington's disease (22). However, at present it is unknown whether loss of functional EAAT2 is the initial mechanism which leads to neuron degeneration or if this loss is secondary to cell death. These issues cannot be easily addressed from human studies. However, the loss of EAAT2 has also been observed in transgenic models of mutant SOD1-mediated ALS (23–25). In *SOD1(G93A)* transgenic mice, EAAT2 protein is progressively decreased in the ventral, but not in the dorsal, horn of the lumbar spinal cord (24). This effect was specifically found in 14- and 18-week-old mice that had motor function impairment, motor neuron loss and reactive astrocytosis. No changes in EAAT2 were observed before the appearance of clinical symptoms. In this study we attempt to supplement the loss of EAAT2 with transgenic EAAT2 and ask whether it can protect neurons from glutamate-induced injury. We generated transgenic mouse lines that express human EAAT2 under the control of the human glial fibrillary acidic protein (GFAP) promoter and then crossed these transgenic mice with *SOD1(G93A)* transgenic mice. Our *EAAT2/SOD1(G93A)* double transgenic mice showed a delay in motor neuron degeneration and the associated motor function at early stage of disease progression but no change in life span when compared to their *SOD1(G93A)* littermates.

RESULTS

Generation and establishment of c-Myc-hEAAT2 transgenic founder mice

We generated transgenic mice expressing human EAAT2 (hEAAT2) under the control of the human glial fibrillary acidic protein (hGFAP) promoter. The GFAP promoter was used in this study because (1) EAAT2 is predominantly expressed in astrocyte and (2) decreases in EAAT2 are accompanied by increased GFAP levels in *SOD1(G93A)* mice (24); the lost EAAT2, therefore, can be supplemented with transgenic hEAAT2. The transgene construct is diagramed in Figure 1A. The 2.2 kb GFAP promoter region has been previously shown to drive high levels of reporter gene expression predominantly in astrocytes beginning during the middle stage of prenatal development and continuing into adulthood (26,27). A c-Myc epitope tag was placed on the N-terminus of hEAAT2 so as to permit detection of transgenic hEAAT2 expression. Transient expression of pcDNA3/c-Myc-hEAAT2 in HEK293 cells showed that the presence of the N-terminal c-Myc epitope tag did not affect the expression, localization and function of hEAAT2 (data not shown). A segment of the mouse protamine-1 (MP1) gene containing an intron and a polyadenylation site was placed on the 3′ end of hEAAT2 cDNA so as to increase expression of the transgene (28).

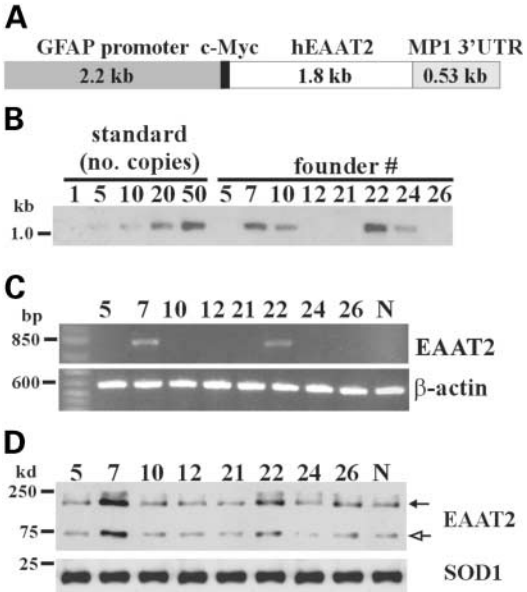

Figure 1. Transgene construct and characterization of the transgenic F0 mice. (**A**) Schematic representation of the GFAP promoter-driven c-Myc-hEAAT2 construct used to generate the transgenic mice. (**B**) Southern blot analysis of transgene copy number. Copy number was estimated by comparing band intensities from each F0 mouse (*founder*) to different copy numbers (*no. copies*) of *Pst*I-digested pGFAP/c-Myc-hEAAT2 (*standard*). Numbers 7 and 22 contained the highest copy numbers. (**C**) RT–PCR analysis of hEAAT2 transgene mRNA expression in brains from the transgenic F0 mice and a non-transgenic littermate (*N*). Mouse β-actin was used as an internal control. Numbers 7 and 22 expressed the highest levels of hEAAT2 mRNA. (**D**) Immunoblot analysis of c-Myc-hEAAT2 protein expression in brains from the transgenic F0 mice and a non-transgenic littermate (*N*) using an antibody against the C-terminus of EAAT2. Both EAAT2 monomer (open arrow) and multimer (filled arrow) bands can be detected with this antibody. Samples of 3 μg of total protein were loaded in each lane. The blots were also probed with an antibody against SOD1 to ensure equal loading of protein. Numbers 7 and 22 showed elevated levels of EAAT2 protein relative to the non-transgenic mice.

The hGFAP-c-Myc-hEAAT2 transgene construct was injected into mouse eggs, which produced 31 F0 mice. The genotyping results by PCR (data not shown) showed that 10 transgenic F0 pups (nos 5, 7, 10, 12, 19, 21, 22, 24, 26 and 32) were obtained. The relative transgene copy number was determined by Southern blot analysis after digestion of genomic DNA with *Pst*I which produces a 1295 bp (from +425 to +1719 of the hEAAT2 cDNA) band in transgenic mice. As shown in Figure 1B, the relative transgene copy numbers differed for each line varying from <5 to 50. The lines 7 and 22 carried more copies of transgene than the other transgenic F0 mice.

Among these 31 F0 pups, three pups were significantly smaller than others. Interestingly, the three smaller mice (nos 19, 22 and 32) were transgenic and carried higher copy numbers of the transgene than the other transgenic mice. These three mice died prematurely (no. 32, 3 weeks; no. 19, 2 months and no. 22, 6 months) compared with the other transgenic F0 mice. The no. 19 female mouse produced one litter and the no. 22 male mouse produced three litters before dying. They produced fewer pups per litter (2–4) and either none or a few of the resultant pups were transgenic. All of the resultant F_1 transgenic pups were unusually small. Of all of the transgenic F_1 pups produced from the no. 22 male founder mouse, only one pup survived to reproductive age. This mouse was then used to maintain the no. 22 line. We also examined embryos at different developmental stages from the no. 22 male transgenic mouse. More than 80% of these embryos carried the transgene, indicating that the transgene integrated into multiple chromosomes in the no. 22 mouse. Before E14.5, the number and the size of embryos were normal ($n = 12$–16 per litter). However, after E14.5, abnormal embryos were observed and the numbers of embryos were dramatically decreased. Interestingly, GFAP expression has been shown to significantly increase from E14.5 (26,27). It is possible that overexpression of EAAT2 may be lethal during embryonic development.

RT–PCR and immunoblot analyses were carried out to determine c-Myc-hEAAT2 transgene expression in each line using non-transgenic littermates as negative controls. RT–PCR results showed that c-Myc-hEAAT2 mRNA could only be detected in line 7 and line 22 (Fig. 1C). Quantitative immunoblot analysis of c-Myc-hEAAT2 protein expression in whole brain extracts of transgenic mice as well as their non-transgenic littermates was performed using antibodies against the C-terminus of EAAT2. We could not detect transgenic protein expression by immunoblot analysis using antibodies against the c-Myc epitope tag (the possible reasons are discussed in the Discussion section); however, these antibodies could detect transgene protein by immunohistochemistry (see below, Fig. 2B). The results (Fig. 1D) showed that increased EAAT2 protein expression in line 7 (2.2-fold) and line 22 (1.8-fold) mice but not in those lines which contain fewer copies of the transgene when compared to non-transgenic littermates. There was no difference in SOD1 protein expression between transgenic and non-transgenic mice.

Expression and localization of c-Myc-hEAAT2 protein in transgenic mice

We determined the expression profile of the c-Myc-hEAAT2 protein in different tissues of adult (2 months) transgenic and non-transgenic littermate mice. c-Myc-hEAAT2 protein could be detected in the brain and spinal cord (Fig. 2A), but not in peripheral tissues such as the kidney, heart and lung (data not shown). Overexpression of c-Myc-hEAAT2 did not alter the protein levels of other glutamate transporters such as EAAT1 or EAAT3 nor SOD1 in the CNS (Fig. 2A shows EAAT1 and SOD1immunoblotting results and EAAT3 is not shown). The localization of c-Myc-hEAAT2 within the CNS was examined in transgenic and non-transgenic mice using antibodies against EAAT2 as well as the c-Myc epitope tag. Increased EAAT2 and c-Myc immunoreactivities were observed in both the brain (data not shown) and spinal cord (Fig. 2B) of transgenic mice when compared with non-transgenic littermates.

In order to verify that c-Myc-hEAAT2 was properly expressed on the surface of transgenic mouse astrocytes, we performed cell surface biotinylation experiments on cortical primary dissociated cultures derived from *c-Myc-hEAAT2* transgenic mice as well as from non-transgenic littermates. The cultures were incubated either with biotin-7-NHS (*Bt*) or with buffer alone (*Non*) followed by cell lysis. The resultant lysates were subjected to avidin affinity chromatography and the avidin-bound proteins (*B*) as well as the unbound proteins (*FT*) were analysed for EAAT2 and SOD1 (a marker for intracellular proteins) locations by immunoblotting. Those proteins which were retained on an avidin column are considered to be the cell surface proteins while the unbound proteins are the intracellular proteins. As shown in Figure 2C, EAAT2 was primarily located at the cell surface fraction (*Bt*) and there was a strong increase (∼2.5-fold) in cell surface EAAT2 in transgenic cultures when compared with non-transgenic cultures. The cytosolic protein SOD1 was only found in the intracellular fractions.

Subcellular fractionation was performed to determine if c-Myc-hEAAT2 is properly localized to the plasma membrane *in vivo*. Transgenic and non-transgenic mouse forebrain homogenates (*H*) were fractionated into plasma membrane (*P*), Golgi apparatus (*G*) and endoplasmic reticulum (*E*) fractions by discontinuous sucrose gradient centrifugation and examined for the expression of EAAT2 and Na^+/K^+ ATPase $\alpha1$ (a marker for plasma membrane-associated proteins) in each of these fractions by immunoblotting. The EAAT2 fractionation profiles were similar between transgenic and non-transgenic forebrain samples (Fig. 2D), indicating that the transgenic c-Myc-hEAAT2 was properly targeted to the plasma membrane. Furthermore, there was a strong increase in EAAT2 protein levels in the P fraction from transgenic mice when compared with non-transgenic littermates. Similar results were obtained with transgenic and nontransgenic spinal cord samples (data not shown). The fractionation profile of the Na^+/K^+ ATPase $\alpha1$ was also similar between transgenic and non-transgenic forebrains, even though the expression of Na^+/K^+ ATPase $\alpha1$ was lower in transgenic mice. The cell surface biotinylation and subcellular fractionation results demonstrate that c-Myc-hEAAT2 is properly localized to the plasma membrane.

Na^+-dependent [^{3}H]glutamate uptake in transgenic synaptosomes

[^{3}H]Glutamate uptake assays were used to determine if overexpression of c-Myc-hEAAT2 enhanced glutamate transport. We measured Na^+-dependent and -independent [^{3}H]glutamate uptake ability in synaptosomal preparations (P2 fractions) from the cerebral cortex (*ctx*), subcortical forebrain (*sctx*), cerebellum (*cb*), brainstem (*bs*) and spinal cord (*sc*) of transgenic mice as well as of their non-transgenic littermates. There was a significant increase in Na^+-dependent [^{3}H]glutamate uptake in transgenic synaptosomes from the

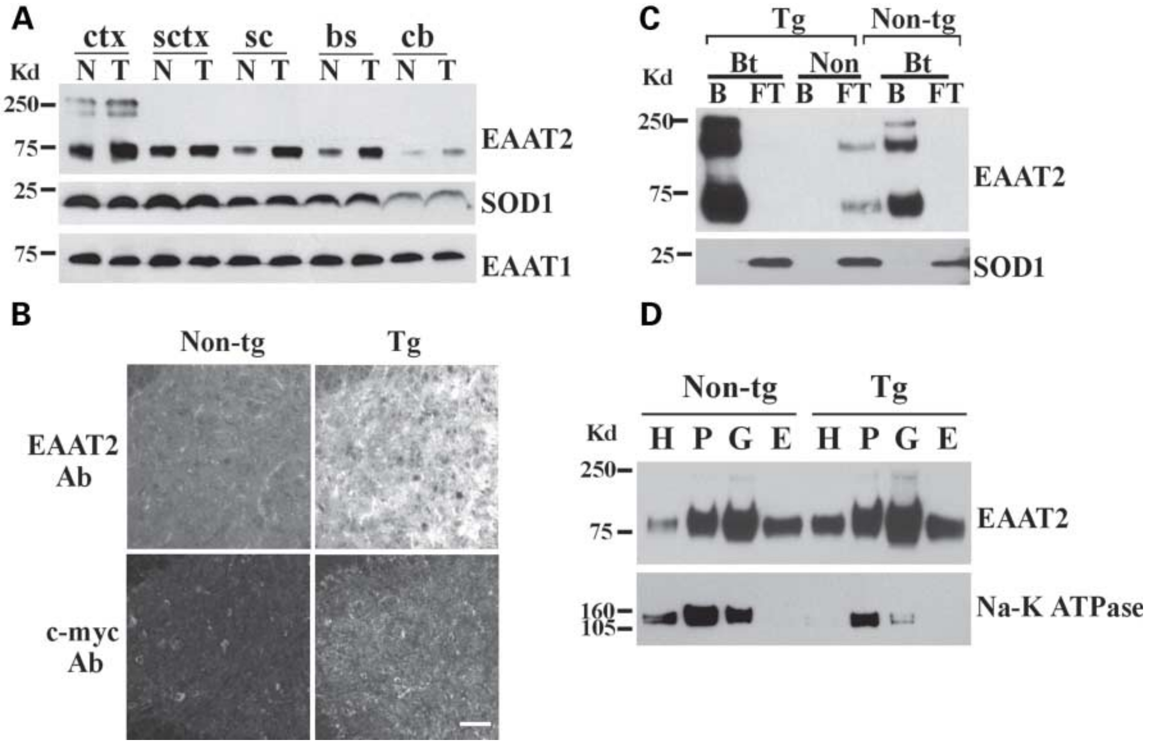

Figure 2. Expression and localization of c-Myc-hEAAT2 protein in transgenic mice. (**A**) Immunoblot analysis of glial glutamate transporters expression in different regions of the adult (2 months) line 7 transgenic mice (*T*) ($n = 3$) and their non-transgenic littermates (*N*) ($n = 3$). SOD1 was used as an internal control for equal loading of protein. For EAAT2 and SOD1 3 µg of total protein were loaded, while 15 µg of protein were loaded for EAAT1. As expected there is a strong increase in EAAT2 protein expression in the transgenic samples, especially in the brainstem and spinal cord. Overexpression of EAAT2 did not alter the expression of EAAT1 nor SOD1 protein in the CNS. *ctx*, cortex; *sctx*, subcortex; *sc*, spinal cord; *bs*, brainstem; *cb*, cerebellum. (**B**) Immunohistochemical localization of c-Myc-hEAAT2 in the ventral horns of transgenic (*Tg*; $n = 3$) and non-transgenic (*Non-tg*) mice ($n = 3$) with either an antibody against EAAT2 or an antibody against the c-Myc epitope tag. Increased EAAT2 and c-Myc immunoreactivities were observed in the ventral horns of transgenic mice. Scale bar, 20 µm. (**C**) Cell surface expression of EAAT2 on transgenic astrocyte cultures. Cell surface biotinylation (*Bt*) was used to label proteins expressed on the cell surfaces of cortical primary dissociated cultures derived from transgenic (*Tg*) and nontransgenic (*Non-tg*) littermates. As a negative control, biotin-7-NHS was omitted (*Non*). Avidin-bound (*B*) proteins as well as the flow-through (*FT*) were analyzed for EAAT2 and SOD1 (a marker for intracellular proteins) expression by immunoblot analysis. 50% of total samples from avidin-bound proteins were loaded in the *B* lanes while 10% of the total flow-throughs were loaded in the *FT* lanes. There was a ~2.5-fold increase in biotinylated EAAT2 in transgenic astrocyte cultures when compared with non-transgenic astrocyte cultures. As expected, SOD1 did not bind to the avidin column showing that the biotinylation reaction was specific to cell surface proteins. (**D**) Subcellular distribution of EAAT2 in transgenic and non-transgenic mouse brains. Homogenates (*H*) from transgenic and non-transgenic mouse forebrains were resolved into plasma membrane (*P*), Golgi apparatus (*G*) and endoplasmic reticulum (*E*) fractions by discontinuous sucrose gradient centrifugation. These fractions were then analyzed for EAAT2 and Na^+/K^+ ATPase $\alpha1$ subunit (a positive control for a membrane-bound protein) protein expression by immunoblot (3 µg of protein were loaded in each lane). There was a strong increase in the expression of EAAT2 in the transgenic mice and the fractionation profile of EAAT2 in transgenic mice was nearly identical to that observed in nontransgenic mice. Likewise, the fractionation profile of the Na^+/K^+ ATPase $\alpha1$ was similar between transgenic and non-transgenic forebrains even though the expression of Na^+/K^+ ATPase $\alpha1$ was lower in transgenic mice.

cerebral cortex (1.5-fold; $P = 0.003$), subcortical forebrain (2.1-fold; $P = 0.0004$), cerebellum (1.4-fold; $P = 0.225$), brainstem (1.4-fold; $P = 0.048$) and spinal cord (2.3-fold; $P = 0.0034$) when compared with corresponding non-transgenic samples (Fig. 3). Na^+-independent [^{3}H]glutamate uptake was not altered in transgenic synaptosomes (data not shown). Overexpression of c-Myc-hEAAT2 increases glutamate uptake in the CNS.

Modulation of glutamate-induced toxicity in cultures derived from transgenic mice

Does increased expression of EAAT2 protect neural cells from excitotoxic damage? We used cortical primary dissociated cultures derived from *c-Myc-hEAAT2* transgenic mice and non-transgenic littermates to examine the effect of c-Myc-hEAAT2 overexpression on glutamate-induced cell damage. The cultures contained ~30% neurons as determined by MAP-2 immunostaining (data not shown). Astrocyte surface EAAT2 expression was increased ~2.5-fold in transgenic cultures when compared with non-transgenic cultures as determined by immunostaining (data not shown) and cell surface biotinylation (Fig. 2C). Na^+-dependent [^{3}H]glutamate uptake was 1.8 ± 0.1-fold ($P = 0.00013$) higher in transgenic cultures as compared with non-transgenic cultures (data not shown). The cultures were exposed to 1 mM sodium L-glutamate (in B-27-free DMEM) or vehicle (1 mM NaCl) for 24 h. Glutamate-mediated cytotoxicity was assessed by measuring lactate dehydrogenase (LDH) activity in the culture media taken at various time points. Dying or dead cells non-specifically release LDH as well as other cytosolic enzymes during the process of cell death (29). Total LDH activity was also measured from Triton X-100-lysed sister cultures so as to normalize the extracellular LDH activity. As shown in Figure 4A, glutamate treatment significantly increased LDH release relative to vehicle treatment, especially at early time points (compare circles with triangles). The observed LDH release increased with time in the vehicle-treated cells could be the result of prolonged B-27 deprivation. Importantly, the amount of LDH release was lower in glutamate-treated transgenic cultures (filled circles) when compared with glutamate-treated non-transgenic cultures (open circles). After subtracting the vehicle-treated LDH release from glutamate-treated LDH release, glutamate-induced LDH release was statistically significantly lower (45–53%, $P < 0.001$) at early time points (<3 h) in transgenic cultures when compared with non-transgenic cultures (Fig. 4B). Direct comparisons of glutamate-induced LDH release between transgenic and nontransgenic cultures could not be made after 3 h since the LDH release in glutamate-treated non-transgenic cultures appeared to reach plateau. These results suggest that overexpression of c-Myc-hEAAT2 protect cultured cells from glutamate-induced cytotoxicity.

We also determined the effect of overexpression of c-Myc-hEAAT2 on glutamate-induced chromatin condensation, a hallmark feature of cell death. The cultures were treated with 1 mM L-glutamate or vehicle for 24 h and then stained with the chromatin-binding dye bis-benzimide (Hoechst 33342; Fig. 4C). The majority of cells that showed condensed chromatin were neurons. Quantitative analysis (Fig. 4D) revealed a statistically significant increase (3.1-fold; $P = 0.0017$) in the relative number of neurons with condensed chromatin in non-transgenic cultures treated with glutamate when compared to vehicle. However, transgenic cultures only experienced a 0.3-fold increase ($P = 0.032$) in the number of cells exhibiting chromatin condensation upon exposure to L-glutamate. These results suggest that overexpression of c-Myc-hEAAT2 in astrocytes protects neurons from glutamate-induced cell death.

Increased expression of EAAT2 improves motor performance but does not delay the onset of paralysis nor prolongs the life span of the *SOD1 (G93A)* transgenic mouse model of ALS

To determine if an increase in EAAT2 expression can prevent or delay the progression of ALS, we crossed heterozygous *c-Myc-hEAAT2* mice (from line 7 and line 22) with heterozygous *SOD1(G93A)* mice which carry a high copy number of the SOD1(G93A) transgene (8). The resultant *c-Myc-hEAAT2:SOD1(G93A)* double transgenic (*G93A/EAAT2*) as well as *c-Myc-hEAAT2* transgenic (*EAAT2*), *SOD1(G93A)* transgenic (*G93A*) and non-transgenic (*non-tg*) mice were then examined for changes in motor performance, the onset of paralysis, body weight and life span. The ratio of males to females was constant for all populations. The *SOD1(G93A)* transgene copy numbers and SOD1(G93A) protein expression levels were not different between *G93A* mice and *G93A/EAAT2* mice as determined by Southern blot analysis and quantitative immunoblot analysis, respectively (data not shown). We first monitored motor performance using a rotorod but the mice could not be trained to remain on the rotorod. Instead, motor performance was assessed by measuring grip strength. There was no difference in grip strength between *EAAT2* transgenic mice and their non-transgenic littermates (data not shown). The *G93A* transgenic mice showed no change in grip strength between 60 and 74 days of age (151.4 ± 28.7 g, $n = 25$); grip strength began to decline by 8.6% decline at 81 days of age (138.3 ± 29.8 g) and this decline continued through 109 days (98.8 ± 20.8 g) at a similar rate (Fig. 5A). On the other hand, the *G93A/EAAT2* mice showed no change in grip strength between 60 and 81 days of age (152.1 ± 31.5 g for line 7, $n = 15$ and 157.6 ± 30.7 g for line 22, $n = 12$) and a 5.5% decline in grip strength at 88 days of age (144.1 ± 27.5 g for line 7 and 149.6 ± 28.4 g for line 22) and continued at a similar rate to 109 days (117.7 ± 29.3 g for line 7 and 122.7 ± 30.1 g for line 22; Fig. 5A). The cumulative probability of onset as defined by the grip strength deficit was significantly delayed (by ~14 days, $P < 0.01$; Fig. 5B) in the *G93A/EAAT2* transgenic mice (95.8 ± 6.8 days for line 7 and 98.3 ± 7.4 days for line 22) when compared with *G93A* mice (82.8 ± 7.6 days). The onset of paralysis was not delayed (Fig. 5C) in the *G93A/EAAT2* mice (110.8 ± 3.2 days for line 7, $n = 15$ and 109.6 ± 7.6 days for line 22, $n = 12$) when compared with *G93A* mice (107.5 ± 4.9 days, $n = 25$). The decline in body weight (Fig. 5D) occurred at the same time in *G93A/EAAT2* mice (107.5 ± 4.7 days for line 7, $n = 15$ and 108.6 ± 3.7 days for line 22, $n = 12$) as in *G93A* mice (105.8 ± 7.4 days, $n = 25$). The mean life span (Fig. 5E) was not significantly different between *G93A/EAAT2* mice (136.1 ± 5.0 days for line 7, $n = 15$ and 132.0 ± 3.7 days for line 22, $n = 12$) and *G93A* mice (132.7 ± 7.4 days, $n = 25$). Taken together, these results indicate that increased expression of hEAAT2 can improve motor performance but has no effect on the progression or the ultimate outcome of the disease in the *G93A* transgenic mouse model of ALS.

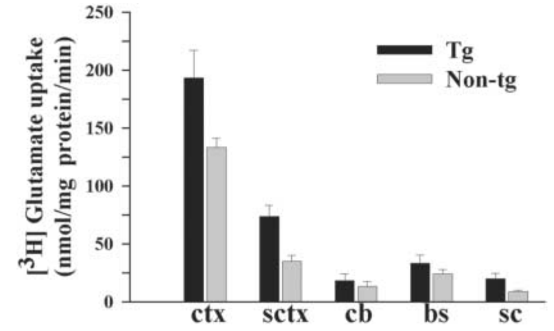

Figure 3. Na^+-dependent $[^3H]$glutamate uptake in synaptosomes from *c-Myc-hEAAT2* transgenic and non-transgenic mice. Synaptosomes (P2 fractions) were prepared from cerebral cortices (*ctx*), subcortical forebrains (*sctx*), cerebella (*cb*), brainstems (*bs*) and spinal cords (*sc*) of *c-Myc-hEAAT2* transgenic (line No. 7; black bars; $n = 6$) and non-transgenic (gray bars) littermates ($n = 6$). These preparations were then analyzed for Na^+-dependent $[^3H]$glutamate uptake. There was a strong increase in Na^+-dependent $[^3H]$glutamate uptake in the cerebral cortices, subcortical forebrains and spinal cords from transgenic mice relative to non-transgenic littermates (*$P < 0.05$; **$P < 0.005$).

Increased expression of c-Myc-hEAAT2 partially protects motor neurons from SOD1(G93A)-mediated degeneration

To determine if increased expression of c-Myc-hEAAT2 would prevent the motor neuron loss observed in the *G93A* mice, we counted the number of motor neurons in the lumbar spinal cord of *G93A* transgenic, *G93A/EAAT2* transgenic and non-transgenic mice at 90 days (early stage of disease progression)

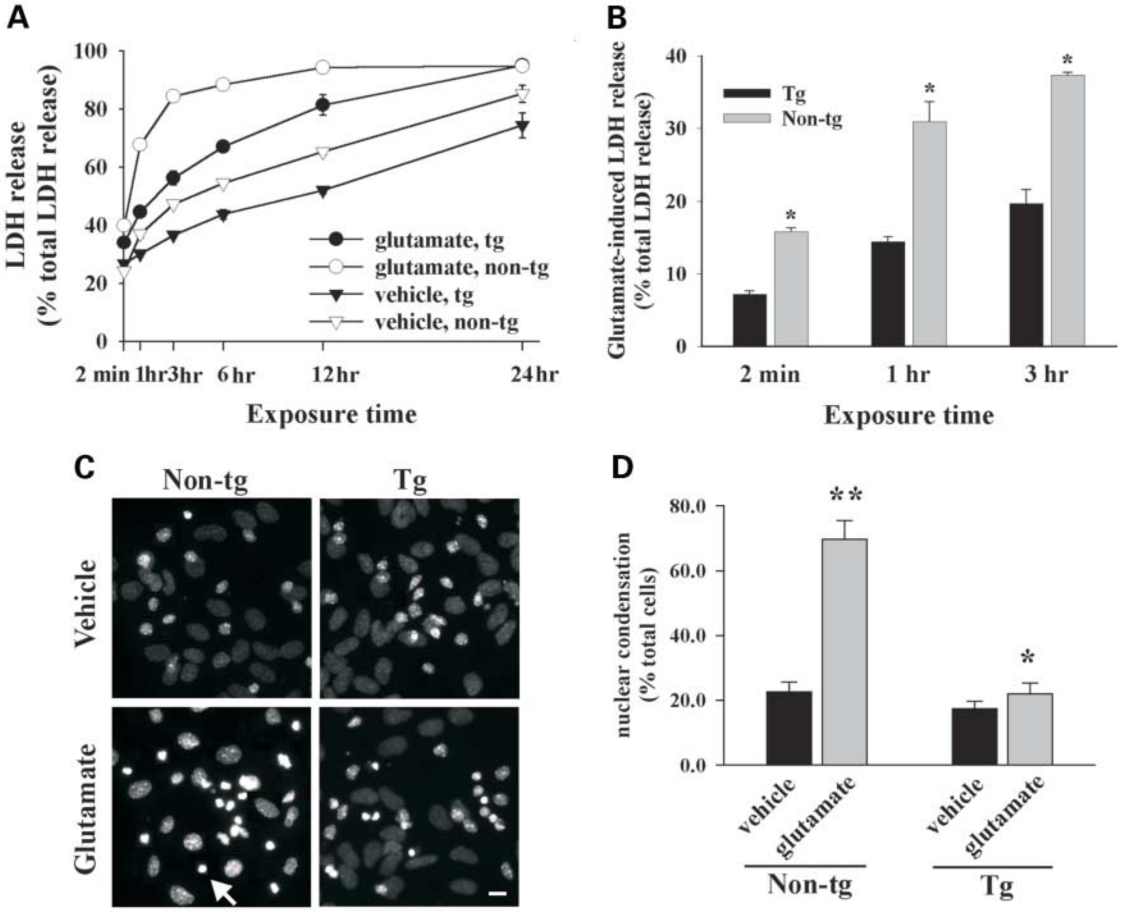

Figure 4. Increased expression of EAAT2 protects cells from glutamate-induced toxicity in cortical primary dissociated cultures. Primary dissociated cultures were prepared from *c-Myc-hEAAT2* transgenic (Tg) and non-transgenic (Non-tg) mouse cortices. (**A**) Glutamate-induced cytotoxicity was assessed using lactate dehydrogenase (LDH) release in cultures following exposure to 1 mM sodium L-glutamate (in B-27-free DMEM, circles, $n = 3$) or vehicle (1 mM NaCl, triangles, $n = 3$) for 2 min to 24 h. LDH release was expressed relative to total LDH release (i.e. from Triton X-100 lysed cells). LDH release was higher in glutamate-treated cultures than in vehicle-treated cultures at all time points tested (compare circles to triangles). Glutamate-induced LDH release was higher in Non-tg cultures than in Tg cultures at the early time points (compare open circles with closed circles). The observed LDH release increased with time in vehicle-treated cultures could be the result of prolonged B-27 deprivation. The experiments were repeated three times with consistent results. (**B**) After subtracting the vehicle-treated LDH release from glutamate-treated LDH release, glutamate-induced LDH release was statistically significantly lower ($^*P < 0.001$) at early time points (<3 h) in transgenic cultures when compared with non-transgenic cultures. (**C**) Representative micrograph of bis-benzimide (Hoechst 33342) stained Tg and Non-tg cultures treated with either 1 mM L-glutamate or vehicle for 24 h. The arrow indicates a cell with condensed chromatin. The small, strongly stained nuclei originate from neurons while the large, lightly stained nuclei originate from flat, polygonal-type astrocytes; these lightly stained cells were not used for quantitative analysis. Scale bar, 10 µm. (**D**) Quantitative analysis of bis-benzimide staining revealed a statistically significant increase in the relative number of neurons with condensed chromatin in non-transgenic cultures (3.1-fold; $^{**}P = 0.0017$) treated with glutamate when compared to vehicle. However, transgenic cultures only experienced a 0.3-fold increase ($^*P = 0.032$) in the number of cells exhibiting chromatin condensation upon exposure to glutamate. $n = 5$ per group with at least 20 neurons per image.

and 110 days (middle stage of disease progression) of age. As shown in Figure 6A and B, about 27.3% of the motor neurons were loss in *G93A* mice at 90 days of age when compared with non-transgenic littermates and only 40.3% of the motor neurons in the lumbar spinal cord remained at 110 days (compare *Wild-type* with *G93A*). The remaining motor neurons in the *G93A* mice were atrophic. In contrast, there was no significant loss of motor neurons in the lumbar spinal cord of *G93A/EAAT2* transgenic mice at 90 days when compared with *G93A* mice; only 38.3% of the motor neurons were lost in the ventral spinal cord of *G93A/EAAT2* transgenic mice at 110 days (compare *G93A/EAAT2* to *G93A*). The motor neurons in the lumbar spinal cord of *G93A/EAAT2* transgenic mice were healthier in appearance than those in the *G93A* transgenic mice. Overexpression of c-Myc-hEAAT2 alone did not result in the loss of motor neurons at 90 days (compare *EAAT2* with *wild-type* at 90 days). Motor neuron loss was not prevented, however, since most of the motor neurons in the *G93A/EAAT2* transgenic mice were lost at ∼130 days (late stage of the disease, data not shown).

We also assessed the effect of c-Myc-hEAAT2 overexpression on axonal degeneration observed in the spinal cord of *G93A* mice. As shown in Figure 6C, degeneration of axons in the ventral root of the spinal cord was evident at 90 days of age in *G93A* mice and most of the ventral root axons had degenerated at 110 days of age (compare *G93A* with *wild-type*). Increased expression of c-Myc-hEAAT2 delayed the degeneration of large axons observed in the *G93A* mice

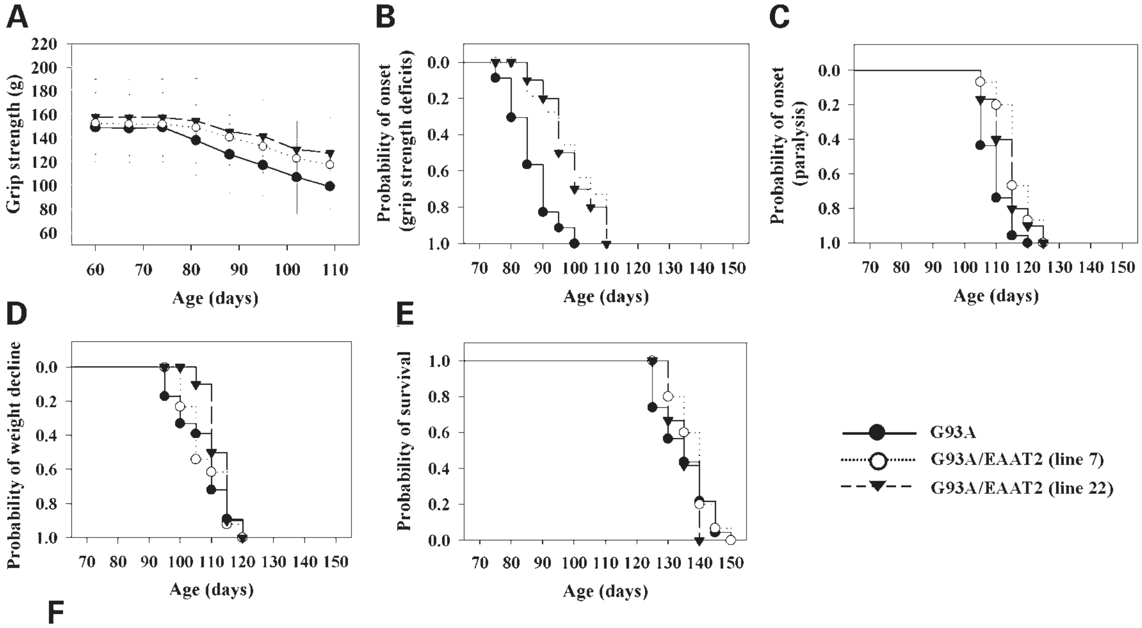

F

	G93A (n=25)	G93A/EAAT2 Line 7 (n=15)	*P* value	G93A/EAAT2 Line 22 (n=12)	*P* value
Grip strength deficient	82.8±7.6 d	95.8±6.8 d	0.007*	98.3±7.4 d	0.004*
Paralysis	107.5±4.9 d	110.8±3.2 d	0.24	109.6±7.6 d	0.31
Weight decline	105.8±7.4 d	107.5±4.7 d	0.49	108.6±3.7 d	0.28
Mortality	132.7±7.4 d	136.1±5.0 d	0.14	132.0±3.7 d	0.91

Figure 5. Increased expression of EAAT2 improves motor performance but does not delay the onset of paralysis nor prolongs the life span of the *SOD1(G93A)* transgenic mouse model of ALS. *G93A* transgenic mice, line 7 *G93A/EAAT2* double transgenic mice and line 22 *G93A/EAAT2* double transgenic mice were analysed for grip strength (indicator of motor performance), onset of paralysis, body weight and life span. The decline in motor performance (**A** and **B**) was significantly delayed (~14 days, $P < 0.01$) in both lines of double transgenic mice when compared to the *G93A* transgenic mouse. However, there were no significant differences in the onset of paralysis (**C**), decline in body weight (**D**) and life span (**E**) between the double transgenic mice and the *G93A* transgenic mice. (**F**) Summary of the statistical analysis of grip strength, onset of paralysis, body weight and life span between *G93A*, line 7 *G93A/EAAT2* and line 22 *G93A/EAAT2* transgenic mice. d, Days

(compare *G93A/EAAT2* with *G93A* at 90 days and 110 days). These results strongly suggest that increased expression of c-Myc-hEAAT2 can partially protect motor neurons from SOD1(G93A)-mediated toxicity.

Effects of c-Myc-hEAAT2 on the loss of EAAT2, gliosis, SOD1 aggregation and caspase-3 activation

To explore possible mechanisms of the neuroprotective effect of c-Myc-hEAAT2 expression against SOD1(G93A)-induced toxicity, we examined the effects of c-Myc-hEAAT2 expression on the occurrence of the following events associated with *G93A* mice: loss of EAAT2 protein (24,25), gliosis (8), SOD1 aggregation (10) and caspase-3 activation (30). Lumbar spinal cords from different ages of mice including 60-day-old (presymptomatic stage), 110-day-old (symptomatic stage) and end stage were used for these experiments. Quantitative immunoblot analysis and immunofluorescent staining were performed. EAAT2 protein levels were gradually lost with disease progression in *G93A* transgenic mice but were gradually accumulated in *G93A/EAAT2* mice (Fig. 7A and B). The increase in EAAT2 protein levels is because expression of *c-Myc-hEAAT2* transgene is under the control of the GFAP promoter and GFAP levels are increased during disease progression. Na^+-dependent [^{3}H]glutamate uptake was examined and showed that glutamate uptakes were decreased with disease progression in *G93A* transgenic mice but were not significantly changed in *G93A/EAAT2* mice (Fig. 7C). These results indicated that our *G93A/EAAT2* mice overexpressed functional transgenic EAAT2 protein during the disease process.

GFAP immunostaining, a marker for reactive gliosis, was not significantly different between *G93A* and *G93A/EAAT2* mice, suggesting that increased expression of EAAT2 does not affect gliosis observed in ALS (Fig. 8A and B).

Consistent with previous findings (10), we also observed an increase in the amount of mutant SOD1 in both *G93A* and *G93A/EAAT2* mice during the disease process, but the increase was less in *G93A/EAAT2* transgenic mice when compared with *G93A* mice as determined by quantitative immunoblot analysis under reducing conditions and immunofluorescent staining (Fig. 8A and B). Immunoblot analysis under non-reducing conditions showed an increase in higher molecular weight (>200 kDa) forms of SOD1-immunoreactive protein (Fig. 8A, open arrow) in *G93A* mice but only an increase in 22 kDa monomeric SOD1 (Fig. 8A, closed arrow) and ~44-kDa forms

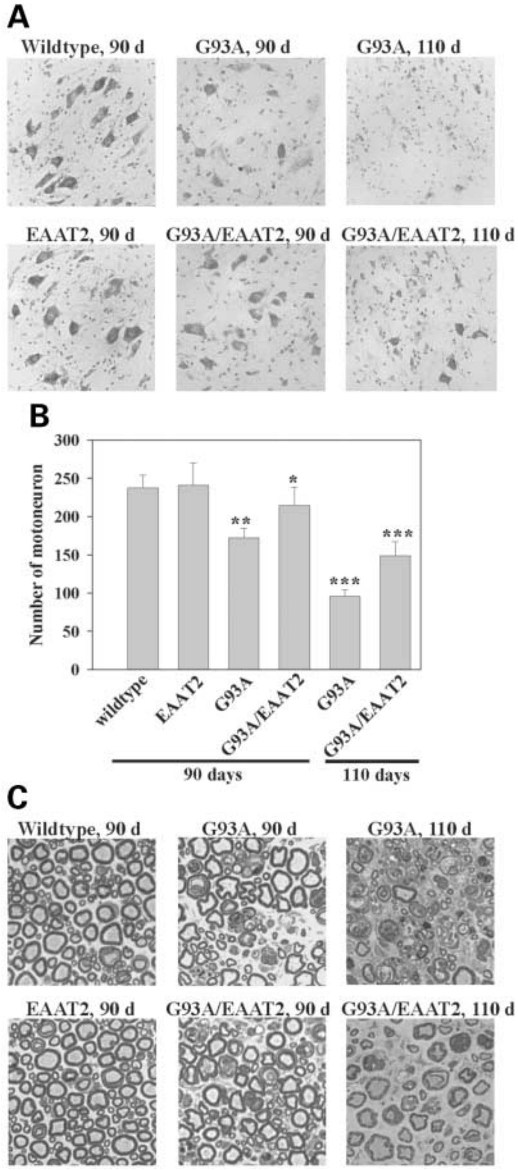
A
Wildtype, 90 d
G93A, 90 d
G93A, 110 d
EAAT2, 90 d
G93A/EAAT2, 90 d
G93A/EAAT2, 110 d
B
Number of motoneuron
300
250
200
150
100
50
0
**
*
***
***
wildtype
EAAT2
G93A
G93A/EAAT2
G93A
G93A/EAAT2
90 days
110 days
C
Wildtype, 90 d
G93A, 90 d
G93A, 110 d
EAAT2, 90 d
G93A/EAAT2, 90 d
G93A/EAAT2, 110 d

Figure 6. Increased expression of c-Myc-hEAAT2 partially protects motor neurons from mutant SOD1-mediated neurodegeneration. (**A**) Cresyl violet staining of the ventral horn of the lumbar spinal cord from non-transgenic (*Wild-type*), *c-Myc-hEAAT2* transgenic (*EAAT2*), *SOD1(G93A)* transgenic (*G93A*) and *c-Myc-hEAAT2: SOD1(G93A)* double transgenic mice (*G93A/EAAT2*). (**B**) Histogram showing the number of motor neurons in *wild-type*, *EAAT2*, *G93A* and *G93A/EAAT2* ventral horns at 90 days and 110 days ($n = 3$ per group). Increased expression of c-Myc-hEAAT2 delayed the progressive loss of motor neurons resulting from the expression of mutant SOD1 (compare *G93A/EAAT2* with *G93A* at 90 and 110 days; $^*P = 0.1$, $^{**}P < 0.001$, $^{***}P < 0.0001$). (**C**) Axonal morphology of ventral horn motor neurons from the lumbar spinal cord of *wild-type*, *EAAT2*, *G93A* and *G93A/EAAT2* mice ($n = 3$ per group). Increased expression of c-Myc-hEAAT2 delayed the degeneration of large axons observed in *G93A* mice (compare *G93A/EAAT2* with *G93A* at 90 days and 110 days).

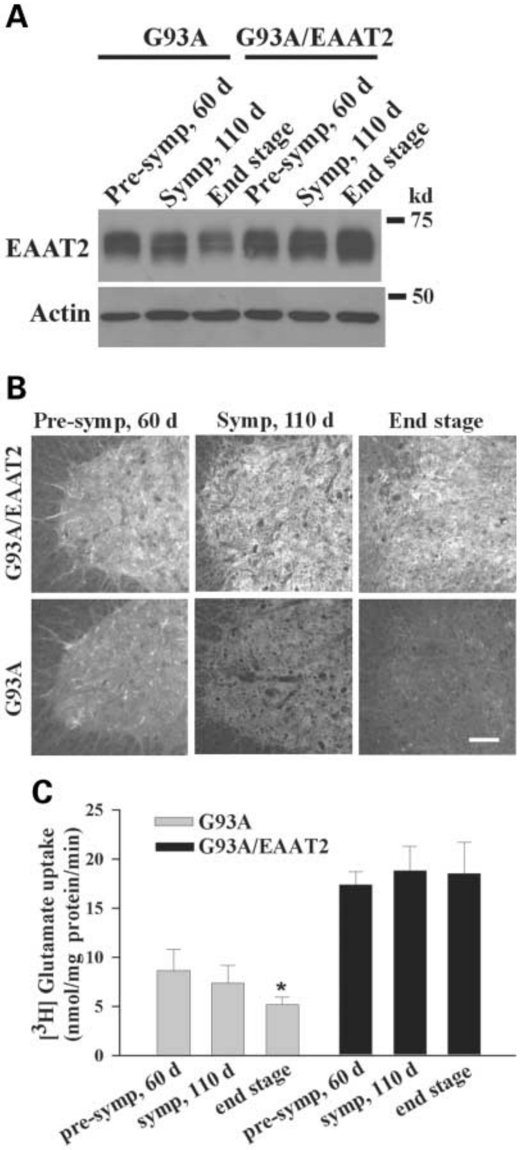
A
G93A
G93A/EAAT2
Pre-symp, 60 d
Symp, 110 d
End stage
Pre-symp, 60 d
Symp, 110 d
End stage
kd
75
EAAT2
50
Actin
B
Pre-symp, 60 d
Symp, 110 d
End stage
G93A/EAAT2
G93A
C
[3H] Glutamate uptake (nmol/mg protein/min)
25
20
15
10
5
0
G93A
G93A/EAAT2
*
pre-symp, 60 d
symp, 110 d
end stage
pre-symp, 60 d
symp, 110 d
end stage

Figure 7. Effect of c-Myc-hEAAT2 on the loss of EAAT2 in the spinal cord of *SOD1(G93A)* transgenic mice. (**A**) Quantitative immunoblot analysis of EAAT2. Lumbar spinal cords from different ages of mice including 60-day-old (presymptomatic stage), 110-day-old (symptomatic stage) and end stage were analysed. Samples of 3 μg total proteins were loaded. The blot was striped and reprobed with anti-actin antibodies to ensure equal loading of protein. EAAT2 protein levels were gradually decreased as disease progression in *G93A* mice but were gradually increased in *G93A/EAAT2* mice. (**B**) Immunostaining of lumbar spinal cord sections with anti-EAAT2 antibodies. Ventral horn regions were shown. Scale bar, 20 μm. (**C**) Na^+-dependent [^{3}H]glutamate uptake in spinal cord synaptosomes. Glutamate uptakes were decreased as disease progression in *G93A* transgenic mice ($^*P < 0.001$), but were not significantly changed in *G93A/EAAT2* mice.

of SOD1-immunoreactive protein (probably dimeric SOD1; Fig. 8A, arrow head) in *G93A/EAAT2* mice at symptomatic and end stage. It is notable that the amount of mutant SOD1 was higher in *G93A* mice than in *G93A/EAAT2* mice (Fig. 8A, SOD1-reducing) but the 22 and ~44 kDa forms of SOD1-immunoreactivity were lower in *G93A* mice (Fig. 8A, SOD1-non-reducing). It is conceivable that there may be very high molecular weight (>250 kDa) forms of SOD1 aggregates that could not enter the gel in *G93A* mice. These results suggest that increased expression of EAAT2 reduces in the formation of high molecular weight forms of SOD1 aggregates.

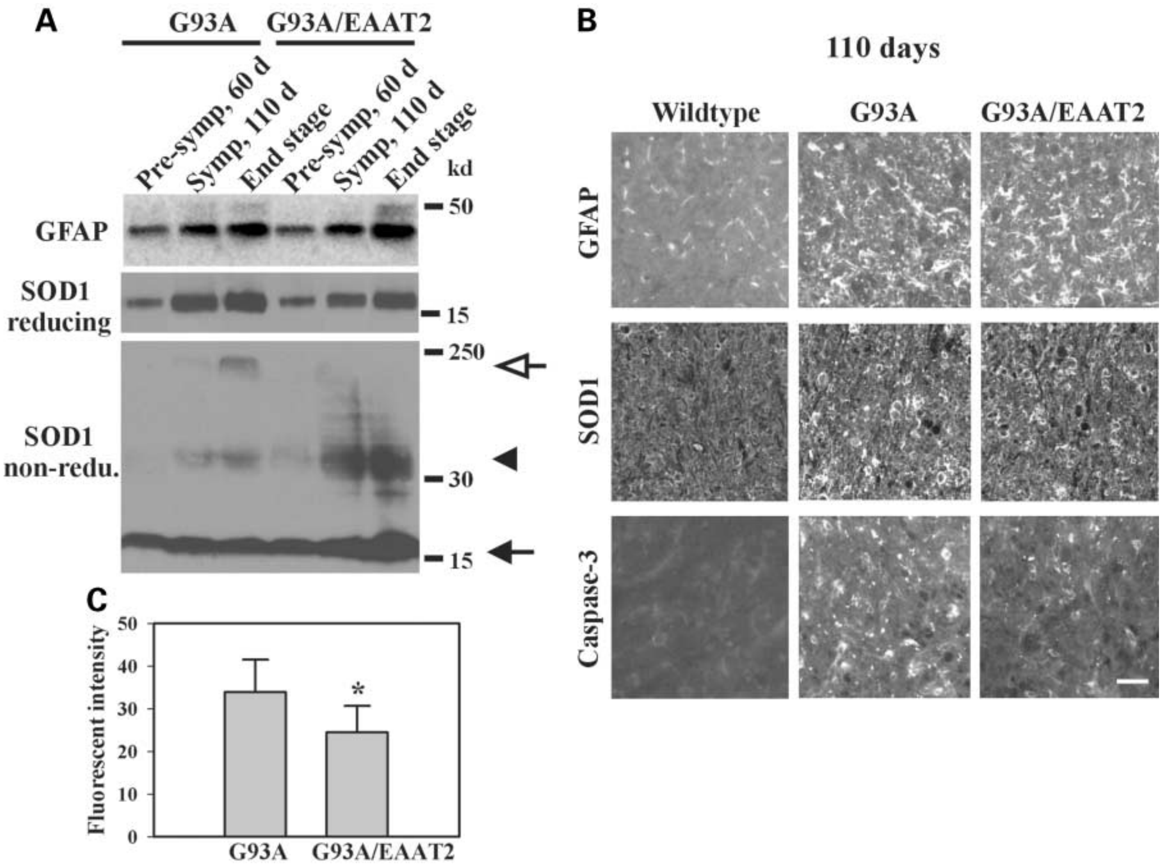

Figure 8. Effect of c-Myc-hEAAT2 on gliosis, SOD1 aggregation and apoptosis in the spinal cord of *SOD1(G93A)* transgenic mice. (**A**) Quantitative immunoblot analysis of GFAP and SOD1 protein levels. Lumbar spinal cords from different ages of mice including 60-day-old (presymptomatic stage), 110-day-old (symptomatic stage) and end stage were analysed. Samples of 5 and 3 µg total protein were loaded for GFAP and SOD1, respectively, and separated by SDS–PAGE under reducing conditions. A 20 µg sample of protein were loaded for SOD1 and separated by SDS–PAGE under non-reducing conditions. GFAP levels were not significantly different between *G93A* and *G93A/EAAT2* mice. An increase in higher molecular weight forms of SOD1 (open arrow) in *G93A* mice but only an increase in 22-kDa monomeric SOD1 (closed arrow) and ~44-kDa forms of SOD1-immunoreactive protein SOD1 (probably dimeric SOD1; arrow head) in *G93A/EAAT2* transgenic mice at symptomatic and end stage. (**B**) Immunostaining of sections from the lumbar spinal cords of mice at 110 days. Ventral horn regions were shown. Scale bar, 10 µm. (**C**) Quantitative analysis of activated caspase-3 immunoreactivity. Fluorescence intensity of caspase-3 immunoreactivity in each motor neuron ($n = 40$) was determined by image analysis using Photoshop (Adobe; *$P < 0.01$). Activation of caspase-3, an indicator of apoptosis, was attenuated in the *G93A/EAAT2* spinal cord compared to *G93A* spinal cord.

For the quantitation of activated caspase-3 levels, we could not obtain reliable results by immunoblot analysis. Quantitative analysis of immunofluorescent staining showed that activated caspase-3 immunoreactivity was statistically significantly reduced (by ~30%, $P < 0.01$) in the lumbar spinal cord of *G93A/EAAT2* transgenic mice when compared to *G93A* mice at 110 days (Fig. 8C). The result was analyzed from 40 motor neurons. Taken together, these results suggest that increased expression of c-Myc-hEAAT2 reduces SOD1(G93A)-induced SOD1 aggregation and caspase-3 activation but not reactive gliosis.

DISCUSSION

In this study we have generated transgenic mice expressing EAAT2 under the control of the GFAP promoter and then crossed these mice with the ALS-associated mutant *SOD1(G93A)* mice to investigate whether supplementation of the loss of EAAT2 that occurs during the disease progression would delay or rescue the disease progression. Our *EAAT2/G93A* double transgenic mice showed a delay (14 days) in grip strength decline but not in the onset of paralysis, body weight decline or life span when compared with *G93A* littermates. We also observed a delay in the loss of motor neurons and their axonal morphologies as well as other events including caspase-3 activation and SOD1 aggregation in our *EAAT2/G93A* mice. This study suggests that the loss of EAAT2 may contribute to, but does not cause, motor neuron degeneration in ALS.

In order to detect transgenic EAAT2 protein expression, we placed a c-Myc epitope tag on N-terminus of EAAT2. However, expression of c-Myc-EAAT2 could not be detected by immunoblotting using anti-c-Myc antibodies obtained from different sources. We believe that it is due to poor antigenicity on N-terminus of EAAT2 protein based on the following observations: (1) we barely detected c-Myc-EAAT2 in

HEK293 cells transfected with pcDNA3-c-Myc-EAAT2 using anti-c-Myc antibodies; (2) we also hardly detected EAAT2 with an N-terminal hemagglutinin (HA) epitope tag using anti-HA antibodies in the transfected HEK293 cells; (3) a rabbit polyclonal antibody directed against N-terminus of EAAT2 cannot easily bind to its antigen (unpublished observations). Nevertheless, we were able to detect c-Myc-EAAT2 by immunohistochemistry using anti-c-Myc antibodies (Fig. 2B). Most importantly, c-Myc-hEAAT2 protein has normal cellular localization and glutamate transport activity as demonstrated in the cultured cells (data not shown) and in the mice (Figs 2 and 3).

The promoter of the human GFAP gene was used in this study to drive expression of the c-Myc-EAAT2 transgene. Interestingly, we observed embryonic lethality or developmental delay and shortened lifespans in the F0 founder mice that carried high copy numbers of the transgene. EAAT2 mRNA is expressed at low levels during the late stages of embryonic development and is significantly increased during postnatal development of the CNS (31). GFAP and reporter genes under the control of the GFAP promoter are expressed during mid-embryonic development (26). Furthermore, ectopically expressed EAAT2 driven by the ubiquitous CMV promoter is toxic to undifferentiated primary astrocytes (32). It is possible, therefore, that inappropriate expression of EAAT2 during development may be detrimental to astrocytes as well as neurons. Further studies will reveal the role of development on the expression of EAAT2 in astrocytes.

One interesting observation from this study is that the expression of the $\alpha1$ subunit of the Na^+/K^+-ATPase was decreased in the *EAAT2* transgenic mice (Fig. 2D). It has been shown that glutamate uptake stimulates Na^+/K^+-ATPase activity in cultured astrocytes (33). This stimulation was the result of activation of a subunit that is highly sensitive to ouabain, i.e. the $\alpha2$ subunit. Interestingly, Na^+/K^+-ATPase $\alpha2$ colocalizes the EAAT2 on the surfaces of astrocytes from the rat somatosensory cortex (34). It is possible that overexpression of EAAT2 and the resultant increase in glutamate uptake may increase the expression of Na^+/K^+-ATPase $\alpha2$ in astrocytes while decreasing the expression of Na^+/K^+-ATPase $\alpha1$. Future studies will determine the involvement of EAAT2 in regulating the Na^+/K^+-ATPase subunit expression profile in astrocytes.

Many studies have examined the importance of glial glutamate transporters in glutamate-induced toxicity. Injections of the glutamate uptake inhibitors dihydrokainate (DHK) and *trans*-pyrrolidine-2,4-dicarboxylate (*trans*-PDC) resulted in neuronal cell loss in the CA1 subfield of the hippocampus (35) and striatum (36). Neuronal degeneration was observed selectively within the hippocampal CA1 subfield of mice with targeted ablation of the *EAAT2* gene (37). Functional knockdown of EAAT2 using antisense oligonucleotides resulted in excitotoxic neurodegeneration in the hippocampus and striatum of rats (15). Furthermore, antisense knockdown of EAAT2 increased the severity of neuronal injury induced by focal cerebral ischemia and traumatic brain injury (38,39). We have shown in this study that increased EAAT2 protein expression protects neurons from the toxic effects of glutamate in primary dissociated cortical cultures derived from transgenic mice (Fig. 4). These studies strongly suggest the importance of EAAT2 function in protecting neurons from excessive levels of extracellular glutamate. The mechanisms by which EAAT2 exerts its protective effect against excitotoxic damage remain to be elucidated.

The loss of functional EAAT2 has been observed in ALS patients as well as in animal models of ALS (18,24,25). However, some groups have reported that EAAT2 levels are unchanged in mice expressing SOD1(G93A) protein (40) and that EAAT2 does not play an early and primary role in the SOD1(G93A)-induced motor neuron death (41). The role of EAAT2 in ALS, therefore, remains controversial. We crossed the *EAAT2* transgenic mice with the *SOD1(G93A)* transgenic mice to investigate whether supplementation of the loss of EAAT2 in *G93A* mice can delay or rescue the disease progression. We have demonstrated that the *G93A/EAAT2* double transgenic mice showed a statistically significant (14 days) delay in grip strength decline when compared with *G93A* littermates (Fig. 5). The delay in onset of grip strength decline was not due to a non-specific effect of overexpression of c-Myc-hEAAT2 since there were no differences in grip strength observed between *EAAT2* transgenic mice and non-transgenic littermates. One may argue that this delay could potentially be due to a strain effect since the *EAAT2* mice were generated in the FVB strain and crossed to the *G93A* mice in the SJL/BL6 hybrid background. We cannot exclude this possibility in the present study. However, the mice used in this study were littermates, which minimizes the genomic background difference. Furthermore, we used a large number of mice and two transgenic lines in this study to strengthen the results. If the observed protective results were due to a strain effect, then our study could suggest that supplementation of the loss of EAAT2 in *G93A* mice cannot change the disease progression and the loss of EAAT2 may be a secondary event resulting from motor neuron degeneration.

We did not observe significant difference in the onset of paralysis, decline of body weight and lifespan between the *G93A/EAAT2* mice and the *G93A* mice in this study (Fig. 5). However, M.L. Sutherland and colleagues (42) have reported that 85% of their *G93A/EAAT2* mice demonstrated delayed onset and life expectancy was increased by 35–40 days compared with *G93A* littermates. The remaining 15% of *G93A/EAAT2* mice demonstrated delayed disease onset and life expectancy was increased by more than 235 days. Both transgenic mice used same human GFAP promoter to drive expression of the EAAT2 transgene. The major difference between these mice is that Sutherland *et al.* overexpressed a fusion protein where a green fluorescence protein (GFP) moiety was placed on the C-terminus of EAAT2 while we overexpressed EAAT2 containing an N-terminal c-Myc epitope tag. Our mice showed an ~2-fold increase in glutamate uptake and their mice showed an ~3-fold increase in glutamate uptake. A systematic comparison of two transgenic lines may elucidate the reasons for the difference in the ability to rescue *G93A* mice from the ALS-like phenotypes between the *EAAT2-GFP* and *c-Myc-EAAT2* transgenic mice.

The most encouraging result in this study is that our *EAAT2/G93A* mice showed a delay in the loss of motor neurons and their axonal morphologies (Fig. 6). These results not only support our grip strength study but also suggest that EAAT2 may play a role in preventing the early stage of

SOD1(G93A)-induced motor neuron degeneration. EAAT2 may protect motor neurons from degeneration by reducing glutamate excitotoxicity or by other unknown mechanisms, which will be investigated in the future.

Bendotti *et al.* (24) have shown that the loss of EAAT2 in *G93A* mice was specifically found in 14- and 18-week-old mice that had motor function impairment, motor neuron loss and reactive astrocytosis. No changes in EAAT2 were observed at 8 weeks of age, i.e. before the appearance of clinical symptoms. Decreases in EAAT2 were accompanied by increased GFAP levels. We also observed the same phenomenon in this study. Interestingly, our EAAT2 transgene was driven by the GFAP promoter; the EAAT2 protein levels in *G93A/EAAT2* mice were gradually increased as GFAP levels elevated during the disease progression (Fig. 7). The lost EAAT2 was supplemented with even more transgenic EAAT2 (Fig. 7). If the hypothesis that loss of EAAT2 leads to an increase of extracellular glutamate level and subsequent neurodegeneration is a primary contributor to disease progression is correct, one would expect to see more profound protective effects. It is notable that the glutamate concentration in the cerebrospinal fluid (CSF) of *G93A* mice was not modified during the disease progression (24). It is possible that loss of EAAT2 is a secondary event to the motor neuron degeneration. One hypothesis could be that the surrounding differentiated astrocytes become undifferentiated when the neurons have degenerated. For unknown reasons, the undifferentiated astrocytes do not express EAAT2 (32). The mechanisms underlying the loss of EAAT2 during the disease progression will be investigated in the future.

Consistent with the delay in the loss of motor neurons, reduced SOD1(G93A)-induced toxic events were observed in the *EAAT2/G93A* mice. Activation of caspases has been shown to occur during the progression of motor neuron degeneration in the *G93A* mouse (30). Intracerebroventricular administration of a broad spectrum caspase inhibitor delayed the onset of ALS and mortality in *G93A* mice (30). Our *EAAT2/G93A* mice showed attenuated caspase-3 activation in the ventral horn of the spinal cord at 110 days when compared to *G93A* littermates (Fig. 8). Furthermore, Bruijn *et al.* (10) observed SOD1-containing inclusion bodies in affected regions from patients with familial ALS as well as from transgenic mice expressing different mutant SOD1 proteins. These SOD1-containing inclusion bodies are present in vimentin-rich aggresomes and are surrounded by abnormal neurofilament deposition in ALS (43). However, the aggregation of SOD1 does not correlate with cell death (44). In this study, we observed reduced in the formation of SOD1 aggregates in our *EAAT2/G93A* double transgenic mice (Fig. 8).

The mechanisms underlying the pathogenesis of selective motor neuron death in ALS are not completely understood and may involve many different components. The loss of glial glutamate transporter function is likely to be a component of the pathogenesis of ALS. This study shows that supplementation of the loss of EAAT2 in *G93A* mice can replenish EAAT2 function, partially prevent motor neuron degeneration and delay the onset of the motor dysfunction, but cannot prolong the life span of these animals. These results suggest that the loss of EAAT2 may contribute to, but does not cause, motor neuron degeneration in ALS.

MATERIALS AND METHODS

Construct design and generation of human EAAT2 transgenic mice

The plasmid DNA containing the complete human EAAT2 cDNA with an N-terminal c-Myc epitope tag (pRK5/c-Myc-hEAAT2) (32) was transiently transfected in HEK293 cells (American Type Culture Collection) (32) to ensure that the cDNA encoded a functional protein. The c-Myc-tagged human EAAT2 cDNA was subcloned from pRK5/c-Myc-hEAAT2 into pGFAP/Lac-1 (26) using *EcoR*I and *BamH*I to generate pGFAP/c-Myc-hEAAT2. The 4.6 kb GFAP/c-Myc-hEAAT2 fragment was excised with *EcoR*I and then injected into FVB/N mouse pronuclei by the Transgenics facility of the Ohio State Neurobiotechnology Center. Integration of the transgene into the FVB/N mouse genome was determined by PCR using genomic DNA extracted from tail biopsies and EAAT2 transgene-specific primers (5′-ggc aac tgg gga tgt aca-3′ corresponding to position +932 from the 5′ translation region and 5′-acg ctg ggg agt tta ttc aag aat-3′ corresponding to position +1738 from the 5′ translation region). PCR conditions were as follows: 95°C for 3 min, 85°C for 2 min; 95°C for 30 s, 55°C for 30 s, 72°C for 1 min for 30 cycles followed by 10 min extension at 72°C. Transgene copy number was determined by Southern blot analysis of *Pst*I-digested tail genomic DNA using a digoxygenin-labeled hEAAT2 cDNA probe as described previously (32). *Pst*I-digested pGFAP/c-Myc-hEAAT2 was used to generate the standard curve.

RT–PCR

Total RNA from mouse brain, spinal cord and other tissues was isolated with TRIzol (Invitrogen; Grand Island, NY, USA) and first-strand cDNA was synthesized with M-MLV reverse transcriptase (Invitrogen) and an EAAT2-specific primer (5′-gga tcc aga ctc ata tcc tta ttt ctc acg-3′ corresponding to position +1708 from the 5′ translation region) as described previously (32). PCR primers and cycle conditions were the same as those used for genotyping. β-Actin was used as an internal control (primers: 5′-cgg gac ctg aca gac tac ctc ctc-3′ corresponding to position +627 from the 5′ translation region and 5′-tgt caa aga aag ggt gta aaa cgc agc-3′ corresponding to position +1250 from the 5′ translation region). PCR conditions were as follows: 94°C for 3 min, 95°C for 1 min, 57°C for 1 min, 72°C for 1 min for 30 cycles followed by 10 min extension at 72°C.

Immunoblotting

Protein extracts were generated from different brain regions and the spinal cord, resolved by SDS–PAGE and transferred onto PVDF membranes as described previously (32). The following primary antibodies were used: rabbit anti-EAAT2 pAb (1:4000; 45), rabbit anti-EAAT1 pAb (1:200) (45), rabbit anti-GFAP pAb (1:1000; Promega), rabbit anti-SOD1 pAb (1:400; Santa Cruz Biotechnology; Santa Cruz, CA, USA), rabbit anti-activated caspase-3 mAb (1:750; clone C92-605, BD Biosciences) and mouse anti-Na^+/K^+ ATPase α1 mAb (1:500; clone α6F) (46). The α6F hybridoma developed by Dr Douglas M. Fambrough was obtained from the Developmental Studies Hybridoma Bank developed under the auspices of the NICHD and maintained by The University of Iowa Department of Biological Sciences. The immunoreactive bands were detected using the SuperSignal West Pico Chemiluminescent Substrate (Pierce Biotechnology) according to the manufacturer's directions. Band intensities were analyzed with Scion Image Release Beta 4.0.2 (Scion Corporation).

[^{3}H]glutamate uptake assay

Uptake of radiolabeled glutamate was monitored in cultured cells and mouse brain synaptosomes as described previously (15,47). Transfected or cultured cells were grown on six-well plates and washed with uptake sample buffer (320 mM sucrose in 50 mM Tris–HCl, pH 7.4) prior to uptake assays. For mouse synaptosomes, mouse brain tissue was homogenized in uptake sample buffer using a Dounce homogenizer and centrifuged at 1000*g* for 10 min at 4°C to remove cellular debris. The supernatant (S1) was then centrifuged at 20 000*g* for 30 min at 4°C and the resultant synaptosome pellet (P2) was resuspended in either Na$^+$-containing or Na$^+$-free Kreb's buffer. Samples were then incubated for 4–10 min at 37°C with 10.2 nML-[^{3}H]glutamate (0.5 µCi; [^{3}H]Glu, Amersham Biosciences, Piscataway, NJ, USA) in either Na$^+$-containing or Na$^+$-free Kreb's buffer supplemented with 40 µM unlabeled glutamate. The cells were washed with ice-cold PBS and then lysed in 1 mM NaOH. The amount of radiolabeled glutamate was measured using a Beckman Coulter LS6500 Multi-Purpose Scintillation Counter (Beckman Instruments, Fullerton, CA, USA). The amount of [^{3}H]Glu transported into the cells was calculated as previously described (47). Na$^+$-dependent [^{3}H]Glu uptake was calculated by subtracting Na$^+$-independent [^{3}H]Glu uptake (in Na$^+$-free Kreb's buffer) from the total [^{3}H]Glu uptake (in Na$^+$-containing Kreb's buffer). Protein concentrations were determined with the Coomassie Plus protein assay (Pierce Biotechnology). Na$^+$-dependent [^{3}H]Glu uptake was expressed as nmol [^{3}H]Glu/mg protein/min.

Immunohistochemistry, immunofluorescence and histology

Fixation of mouse tissue and immunohistochemistry was accomplished as described previously (47) except that the section thickness was 30 µm and the sections were blocked in 3% normal goat serum for 3 h. Immunofluorescent staining of cultured cells was accomplished as described previously (32). The following primary antibodies were used in this study: rabbit anti-EAAT2 pAb (1:1000), rabbit anti-GFAP pAb (1:1000), rabbit anti-SOD1 pAb (1:200), rabbit anti-activated caspase-3 mAb (1:500) and rabbit anti-c-Myc epitope tag pAb (1:100; Affinity BioReagents). Images were obtained using a Zeiss Axioskop 2 upright microscope and AxioVision software.

For motor neuron counting, the L5 root of the spinal cord was dissected and fixed overnight with 4% paraformalehyde in PBS. After postfixing with osmium tetraoxide, roots were dehydrated and embedded in Epon812. Embedded roots were sectioned (1 µm) and stained with toluidine blue. The morphology was examined under a light microscope.

Mouse cortical primary cultures

Cortical neurons and astrocytes were cocultured from newborn (12–24 h) non-transgenic and transgenic pups. The cortices were dissected out of the brains, incubated in activated papain for 30 min at 37°C, triturated by repeated pipetting with a small bore pipette and plated onto poly-D-lysine (1 mg/ml)-coated plastic culture dishes or glass slides. These cultures were maintained in Dulbecco's modified Eagle media (Invitrogen; Grand Island, NY, USA) containing 25 mM glucose, 1 mM sodium pyruvate, 19.4 µM pyridoxine hydrochloride, 2 mM glutamine and 1% B-27 supplement (Invitrogen) until use.

Cell surface biotinylation

Labeling of proteins on the plasma membrane was accomplished by cell surface biotinylation as described previously (48). Cells were washed twice with PBS/CaMg (100 µM $CaCl_2$ and 1 mM $MgCl_2$ in PBS, pH 7.4) at room temperature and then incubated with Biotinylation buffer (1 mg/ml D-biotinyl-ε-aminocaproic acid *N*-hydroxysuccinimide ester (biotin-7-NHS; Roche Applied Science; in PBS/CaMg) for 20 min at 4°C with constant shaking. Cells were then incubated with Quenching buffer (100 mM glycine in PBS/CaMg) for 45 min at 4°C with constant shaking and then incubated with Lysis Buffer (1% Triton X-100 and Complete protease inhibitor cocktail; Roche Applied Science; in PBS, pH 7.4) for 30 min at 4°C with constant shaking. Biotinylated proteins were recovered by incubation with 100 µl immobilized NeutrAvidin (50% slurry; Pierce Biotechnology) at 4°C overnight with end-over-end rotation. The avidin beads were recovered by centrifugation (12 000*g* for 5 min at 4°C) and then washed four times with Lysis Buffer. After washing, the beads were resuspended in 1 × reducing SDS dye.

Subcellular fractionation

Plasma membrane, Golgi apparatus and endoplasmic reticulum fractions were isolated from adult mouse forebrains by discontinuous sucrose gradient centrifugation (49). Briefly, samples were homogenized in Homogenization Buffer (250 mM sucrose and Complete protease inhibitor cocktail in 10 mM Tris–HCl, pH 7.4) using a Dounce homogenizer (20 passes) and a 22-gage needle. Cellular debris was removed by centrifugation at 500*g* for 15 min at 4°C. The homogenates were diluted to 3 mg/ml protein and mixed with an equal volume of 2.3 M sucrose (in 2 M EDTA and 10 mM TrisHCl, pH 7.4). A five-step sucrose gradient was generated (0.33 mL 2.0 M sucrose, 0.67 ml 1.6 M sucrose, 1.33 ml sample (1.4 M sucrose), 1.33 ml 1.2 M sucrose and 0.33 ml 0.8 M sucrose) and centrifuged at 84 210*g* for 62.5 min at 4°C in a SW60 rotor (Beckman Coulter). Ten 400 µl fractions were taken from each sample.

Cytotoxicity assay

Cytotoxicity was assessed by measuring the amount of lactate dehydrogenase (LDH) released from the cells following treatment. Aliquots of culture media were removed from wells at various time points after treatment. Culture media (50 µl/reaction) was mixed with an equal volume of substrate mixture

[25 mM sodium lactate, 3.76 mM β-NAD$^+$ (nicotinamide adenine dinucleotide), 603.4 μM MTT (3-[4,5-dimethylthiazol-2-yl]-2,5-diphenyltetrazolium bromide), 100 μM MPMS (1-methoxyphenazine methosulfate) and 0.1% Triton X-100 in 200 mM Tris–HCl, pH 8.0] and incubated for 30 min at 37°C. The reaction was stopped by adding 100 μl stop solution (20% SDS in 50% dimethylformamide). Absorbance readings were obtained with a GENios microplate reader (Tecan Co., San Jose, CA, USA; $\lambda_{ex} = 570$ nm). Total LDH release was defined as the absorbance from samples of sister cultures lysed with 1% Triton X-100 for 60 min. LDH release in treated cells was expressed relative to total LDH release.

Bis-benzimide staining

Mouse cortical primary cultures were grown on glass coverslips and were processed as described above. The coverslips were incubated with 1 μg/ml bis-benzimide (Hoechst 33342; Molecular Probes) in PBS + BSA for 60 min at room temperature and then washed extensively with PBS + BSA. Coverslips were then mounted onto glass slides with ImmuMount (Shandon Lipshaw). Images were obtained using a Zeiss Axioskop 2 inverted microscope and AxioVision software.

Generation of *hEAAT2:SOD1(G93A)* double transgenic mice

The *hEAAT2* transgenic mice were mated with *SOD1(G93A)* transgenic mice (8) to generate *hEAAT2:SOD1(G93A)* double transgenic mice. *SOD1(G93A)* transgenic mice were obtained from Jackson Laboratories (Bar Harbor, ME, USA). Double transgenic mice were identified by genotyping for hEAAT2 and hSOD1. PCR primers and cycle conditions for EAAT2 were the same as those used for genotyping. The primers for SOD1 were 5′-ctg gca aaa tac agg tca ttg aaa cag aca-3′ corresponding to position +670 from the 5′ translation region and 5′-cag cgt ctg ggg ttt ccg ttg-3′ corresponding to position −63 from the 5′ translation region and PCR condition was 94°C for 3 min, 95°C for 30 s, 52°C for 45 s, 72°C for 1 min for 30 cycles followed by 10 min extension at 72°C.

Phenotype analysis

Neuromuscular performance was used to determine the onset of symptoms and subsequent progression to terminal disease stage of *hEAAT2:SOD1(G93A)* double transgenic mice. An objective assessment of neuromuscular performance was obtained by measuring peak force generated using a Digital Grip Strength Meter outfitted with a Hind Limb Pull Bar Assembly (Columbus Instruments). Five repetitions were taken and the average determined for each mouse. The examiner was unaware of the genotypes of the mice during measurement. Measurements were taken once a week once the animals reached an age of 60 days. Measurements were taken on the same day of the week and at the same time of day; furthermore, all mice were measured within 2 h of each other. Mouse weight was measured with a triple beam balance (Ohaus) immediately after measurement of grip strength. Paralysis onset was scored visually upon the first sign of an abnormal gait indicating muscle weakness. Visual scoring was done three times weekly until onset was detected. To minimize pain or distress, transgenic mice were euthanized when they were unable to right themselves within 30 s when placed on their sides (end-stage of disease).

Statistical analysis

The quantitative data in this study were expressed as the mean ± SEM. Statistical analysis was performed using the unpaired Student's t-test and the ANOVA.

ACKNOWLEDGEMENTS

We thank Dr Arthur Burghes for access to the Grip Strength Meter, Dr Jan Parker-Thornburg for generating transgenic mice, Dr Jeffrey Rothstein for the glutamate transporter antibodies and vigorous discussion, Dr Michael Brenner for the GFAP promoter construct, Dr James King for access to the microscope, Dr Philip Wong for vigorous discussion and Ms Kathleen Wolken and Barbara Diener-Phelan for technical assistance. This work was supported by the NIH (grant MH59805), the ALS Association and the Alzheimer's Association.

REFERENCES

1. Sattler, R. and Tymianski, M. (2001) Molecular mechanisms of glutamate receptor-mediated excitotoxic neuronal cell death. *Mol. Neurobiol.*, **24**, 107–129.
2. Portera-Cailliau, C., Price, D.L. and Martin, L.J. (1997) Excitotoxic neuronal death in the immature brain is an apoptosis-necrosis morphological continuum. *J. Comp. Neurol.*, **378**, 70–87.
3. Portera-Cailliau, C., Price, D.L. and Martin, L.J. (1997) Non-NMDA and NMDA receptor-mediated excitotoxic neuronal deaths in adult brain are morphologically distinct: further evidence for an apoptosis-necrosis continuum. *J. Comp. Neurol.*, **378**, 88–104.
4. Martin, L.J., Price, A.C., Kaiser, A., Shaikh, A.Y. and Liu, Z. (2000) Mechanisms for neuronal degeneration in amyotrophic lateral sclerosis and in models of motor neuron death. *Int. J. Mol. Med.*, **5**, 3–13.
5. Brown, R.H., Jr (1996) Superoxide dismutase and familial amyotrophic lateral sclerosis: new insights into mechanisms and treatments. *Ann. Neurol.*, **39**, 145–146.
6. Siddique, T. and Deng, H.X. (1996) Genetics of amyotrophic lateral sclerosis. *Hum. Mol. Genet.*, **5**, 1465–1470.
7. Przedborski, S., Mitsumoto, H. and Rowland, L.P. (2003) Recent advances in amyotrophic lateral sclerosis research. *Curr. Neurol. Neurosci. Rep.*, **3**, 70–77.
8. Gurney, M.E., Pu, H., Chiu, A.Y., Dal Canto, M.C., Polchow, C.Y., Alexander, D.D., Caliendo, J., Hentati, A., Kwon, Y.W., Deng, H.X. *et al.* (1994) Motor neuron degeneration in mice that express a human Cu,Zn superoxide dismutase mutation. *Science*, **264**, 1772–1775.
9. Wong, P.C., Pardo, C.A., Borchelt, D.R., Lee, M.K., Copeland, N.G., Jenkins, N.A., Sisodia, S.S., Cleveland, D.W. and Price, D.L. (1995) An adverse property of familial ALS-linked SOD1 mutation causes motor neuron disease characterized by vaculolar degeneration of mitochondria. *Neuron*, **14**, 1105–1116.
10. Bruijn, L.I., Houseweart, M.K., Kato, S., Anderson, K.L., Anderson, S.D., Ohama, E., Reaume, A.G., Scott, R.W. and Cleveland, D.W. (1998) Aggregation and motor neuron toxicity of an ALS-linked SOD1 mutant independent from wild-type SOD1. *Science*, **281**, 1851–1854.
11. Dal Canto, M.C. and Gurney, M.E. (1995) Neuropathological changes in two lines of mice carrying a transgene for mutant human Cu,Zn SOD, and in mice overexpressing wild type human SOD: a model of familial amyotrophic lateral sclerosis (FALS). *Brain Res.*, **676**, 25–40.

12. Cleveland, D.W., Bruijn, L.I., Wong, P.C., Marszalek, J.R., Vechio, J.D., Lee, M.K., Xu, X.S., Borchelt, D.R., Sisodia, S.S. and Price, D.L. (1996) Mechanisms of selective motor neuron death in transgenic mouse models of motor neuron disease. *Neurology*, **47**, S54–61.
13. Shaw, C.A. and Bains, J.S. (2002) Synergistic versus antagonistic actions of glutamate and glutathione: the role of excitotoxicity and oxidative stress in neuronal disease. *Cell. Mol. Biol.*, **48**, 127–136.
14. Danbolt, N.C. (2001) Glutamate uptake. *Prog. Neurobiol.*, **65**, 1–105.
15. Rothstein, J.D., Dykes-Hoberg, M., Pardo, C.A., Bristol, L.A., Jin, L., Kuncl, R.W., Kanai, Y., Hediger, M.A., Wang, Y., Schielke, J.P. and Welty, D.F. (1996) Knockout of glutamate transporters reveals a major role for astroglial transport in excitotoxicity and clearance of glutamate. *Neuron*, **16**, 675–686.
16. Rothstein, J.D., Tsai, G., Kuncl, R.W., Clawson, L., Cornblath, D.R., Drachman, D.B., Pestronk, A., Stauch, B.L. and Coyle, J.T. (1990) Abnormal excitatory amino acid metabolism in amyotrophic lateral sclerosis. *Ann. Neurol.*, **28**, 18–25.
17. Rothstein, J.D., Martin, L.J. and Kuncl, R.W. (1992) Decreased glutamate transport by the brain and spinal cord in amyotrophic lateral sclerosis. *New Engl. J. Med.*, **326**, 1464–1468.
18. Rothstein, J.D., Van Kammen, M., Levey, A.I., Martin, L.J. and Kuncl, R.W. (1995) Selective loss of glial glutamate transporter GLT-1 in amyotrophic lateral sclerosis. *Ann. Neurol.*, **38**, 73–84.
19. Lin, C.G., Bristol, L.A., Jin, L., Dykes-Hoberg, M., Crawford, T., Clawson, L. and Rothstein, J.D. (1998) Aberrant RNA processing in a neurodegenerative disease: the cause for absent EAAT2, a glutamate transporter, in amyotrophic lateral sclerosis. *Neuron*, **20**, 589–602.
20. Masliah, E., Alford, M., DeTeresa, R., Mallory, M. and Hansen, L. (1996) Deficient glutamate transport is associated with neurodegeneration in Alzheimer's disease. *Ann. Neurol.*, **40**, 759–766.
21. Li, S., Mallory, M., Alford, M., Tanaka, S. and Masliah, E. (1997) Glutamate transporter alterations in Alzheimer disease are possibly associated with abnormal APP expression. *J. Neuropathol. Exp. Neurol.*, **56**, 901–911.
22. Behrens, P.F., Franz, P., Woodman, B., Lindenberg, K.S. and Landwehrmeyer, G.B. (2002) Impaired glutamate transport and glutamate–glutamine cycling: downstream effects of the Huntington mutation. *Brain*, **125**, 1908–1922.
23. Bruijn, L.I., Becher, M.W., Lee, M.K., Anderson, K.L., Jenkins, N.A., Copeland, N.G., Sisodia, S.S., Rothstein, J.D., Borchelt, D.R., Price, D.L. and Cleveland, D.W. (1997) ALS-linked SOD1 mutant G85R mediates damage to astrocytes and promotes rapidly progressive disease with SOD1-containing inclusions. *Neuron*, **18**, 327–338.
24. Bendotti, C., Tortarolo, M., Suchak, S.K., Calvaresi, N., Carvelli, L., Bastone, A., Rizzi, M., Rattray, M. and Mennini, T. (2001) Transgenic SOD1 G93A mice develop reduced GLT-1 in spinal cord without alterations in cerebrospinal fluid glutamate levels. *J. Neurochem.*, **79**, 737–746.
25. Howland, D.S., Liu, J., She, Y., Goad, B., Maragakis, N.J., Kim, B., Erickson, J., Kulik, J., DeVito, L., Psaltis, G. *et al.* (2002) Focal loss of the glutamate transporter EAAT2 in a transgenic rat model of SOD1 mutant-mediated amyotrophic lateral sclerosis (ALS). *Proc. Natl Acad. Sci. USA*, **99**, 1604–1609.
26. Brenner, M., Kisseberth, W.C., Su, Y., Besnard, F. and Messing, A. (1994) GFAP promoter directs astrocyte-specific expression in transgenic mice. *J. Neurosci.*, **14**, 1030–1037.
27. Andræ, J., Bongcam-Rudloff, E., Hansson, I., Lendahl, U., Westermark, B. and Nistér, M. (2001) A 1.8 kb GFAP-promoter fragment is active in specific regions of the embryonic CNS. *Mech. Dev.*, **107**, 181–185.
28. Braun, R.E., Peschon, J.J., Behringer, R.R., Brinster, R.L. and Palmiter, R.D. (1989) Protamine 3′-untranslated sequences regulate temporal translational control and subcellular localization of growth hormone in spermatids of transgenic mice. *Genes Dev.*, **3**, 793–802.
29. Koh, J.Y. and Choi, D.W. (1987) Quantitative determination of glutamate mediated cortical neuronal injury in cell culture by lactate dehydrogenase efflux assay. *J. Neurosci. Meth.*, **20**, 83–90.
30. Li, M., Ona, V.O., Guegan, C., Chen, M., Jackson-Lewis, V., Andrews, L.J., Olszewski, A.J., Stieg, P.E., Lee, J.P., Przedborski, S. and Friedlander, R.M. (2000) Functional role of caspase-1 and caspase-3 in an ALS transgenic mouse model. *Science*, **288**, 335–359.
31. Sutherland, M.L., Delaney, T.A. and Noebels, J.L. (1996) Glutamate transporter mRNA expression in proliferative zones of the developing and adult murine CNS. *J. Neurosci.*, **16**, 2191–2207.
32. Guo, H., Lai, L., Butchbach, M.E.R. and Lin, C.G. (2002) Human glioma cells and undifferentiated primary astrocytes that express aberrant EAAT2 mRNA inhibit normal EAAT2 protein expression and prevent cell death. *Mol. Cell. Neurosci.*, **21**, 546–560.
33. Pellerin, L. and Magistretti, J.P. (1997) Glutamate uptake stimulates Na^+, K^+-ATPase activity in astrocytes via activation of a distinct subunit highly sensitive to ouabain. *J. Neurochem.*, **69**, 2132–2137.
34. Cholet, N., Pellerin, L., Magistretti, J.P. and Hamel, E. (2002) Similar perisynaptic glial localization for the Na^+, K^+-ATPase $\alpha2$ subunit and the glutamate transporters GLAST and GLT-1 in the rat somatosensory cortex. *Cereb. Cortex*, **12**, 515–525.
35. Arias, C., Arrieta, I., Massieu, L. and Tapia, R. (1997) Neuronal damage and MAP2 changes induced by the glutamate transport inhibitor dihydrokainate and by kainate in rat hippocampus *in vivo*. *Exp. Brain Res.*, **116**, 467–476.
36. Liévens, J.C., Dutertre, M., Forni, C., Salin, P. and Kerkerian-Le Goff, L. (1997) Continuous administration of the glutamate uptake inhibitor L-*trans*-pyrrolidine-2,4-dicarboxylate produces striatal lesions. *Mol. Brain Res.*, **50**, 181–189.
37. Tanaka, K., Watase, K., Manabe, T., Yamada, K., Watanabe, M., Takahashi, K., Iwama, H., Nishikawa, T., Ichihara, N., Kikuchi, T. *et al.* (1997) Epilepsy and exacerbation of brain injury in mice lacking the glutamate transporter GLT-1. *Science*, **276**, 1699–1702.
38. Rao, V.L.R., Dogan, A., Bowen, K.K., Todd, K.G. and Dempsey, R.J. (2001) Antisense knockdown of the glial glutamate transporter GLT-1 exacerbates hippocampal neuronal damage following traumatic injury to rat brain. *Eur. J. Neurosci.*, **13**, 119–128.
39. Rao, V.L.R., Dogan, A., Todd, K.G., Bowen, K.K., Kim, B.T., Rothstein, J.D. and Depsey, R.J. (2001) Antisense knockdown of the glial glutamate transporter GLT-1, but not the neuronal glutamate transporter EAAC1, exacerbates transient focal cerebral ischemia-induced neuronal damage in rat brain. *J. Neurosci.*, **21**, 1876–1883.
40. Deitch, J.S., Alexander, G.M., Del Valle, L. and Heiman-Patterson, T.D. (2002) GLT-1 glutamate transporter levels are unchanged in mice expressing G93A human mutant SOD1. *J. Neurol. Sci.*, **193**, 117–126.
41. Warita, H., Manabe, Y., Murakami, T., Shiote, M., Shiro, Y., Hayashi, T., Nagano, I., Shoji, M. and Abe, K. (2002) Tardive decrease of astrocytic glutamate transporter protein in transgenic mice with ALS-linked mutant SOD1. *Neurol. Res.*, **24**, 577–581.
42. Sutherland, M.L., Martinowich, K. and Rothstein, J.D. (2001) EAAT2 overexpression plays a neuroprotective role in the SOD1 G93A model of amyotrophic lateral sclerosis (ALS). *Soc. Neurosci. Abs.*, **27**, 607.6
43. Johnston, J.A., Dalton, M.J., Gurney, M.E. and Kopito, R.R. (2000) Formation of high molecular weight complexes of mutant Cu, Zn-superoxide dismutase in a mouse model for familial amyotrophic lateral sclerosis. *Proc. Natl Acad. Sci. USA*, **97**, 12571–12576.
44. Lee, J.P., Gerin, C., Bindokas, V.P., Miller, R., Ghadge, G. and Roos, R.P. (2002) No correlation between aggregates of Cu/Zn superoxide dismutase and cell death in familial amyotrophic lateral sclerosis. *J. Neurochem.*, **82**, 1229–1238.
45. Rothstein, J.D., Martin, L., Levey, A.I., Dykes-Hoberg, M., Jin, L., Wu, D., Nash, N. and Kuncl, R.W. (1994) Localization of neuronal and glial glutamate transporters. *Neuron*, **13**, 713–725.
46. Takeyasu, K., Tamkun, M.M., Renaud, K.J. and Fambrough, D.M. (1988) Ouabain-sensitive (Na^+, K^+)-ATPase activity expressed in mouse L cells by transfection with DNA encoding the α-subunit of an avian sodium pump. *J. Biol. Chem.*, **283**, 4347–4354.
47. Butchbach, M.E.R., Lai, L. and Lin, C.G. (2002) Molecular cloning, gene structure, expression profile and functional characterization of the mouse glutamate transporter (EAAT3) interacting protein GTRAP3-18. *Gene*, **292**, 81–90.
48. Daniels, G.M. and Amara, S.G. (1998) Selective labeling of neurotransmitter transporters at the cell surface. *Meth. Enzymol.*, **296**, 307–318.
49. Ma, T., Frigeri, A., Tsai, S.T., Verbavatz, J.M. and Verkman, A.S. (1993) Localization and functional analysis of CHIP28k water channels in stably transfected Chinese hamster ovary cells. *J. Biol. Chem.*, **268**, 22756–22764.